

# Preparation of Ni-Co selenide as long-cycling electrode material of supercapacitor

MIN QIN, SHENGLI XIE\*, YANFENG ZHU, XIAOTONG XU, JIANXIA GOU\*

*College of Chemical Engineering and Safety, Binzhou University, Binzhou 256603, PR China*

Transition metal selenide as supercapacitor electrode materials has been extensively studied and exhibits promising electrochemical performance. However, the poor cycling durability affects its practical application. Here, a design for the fabrication of nickel-cobalt selenide is presented. ZIF-67 was firstly synthesized and then the Ni element was introduced to fabricate precursor, which was then converted into selenides by hydrothermal reaction, in the presence of selenium powder and sodium borohydride. Results show that molar ratio of Co/Ni influences the crystalline phase, particles dispersion state and properties of the obtained selenides. The selenide obtained at optimized molar ratio of Co/Ni (1/1) shows high specific capacitance ( $1234.2 \text{ F g}^{-1}$  at current density of  $1 \text{ A g}^{-1}$ ) and excellent cycling durability (76.0 % of the specific capacitance after 10000 cycles). The outstanding performance may be due to the proper composition and microstructure brought out by the proper Co and Ni molar ratio.

(Received February 15, 2022; accepted June 6, 2022)

*Keywords:* Nickel-cobalt selenide, Supercapacitor, Electrochemical properties

## 1. Introduction

With the rapid development of economy, the energy demand increases. While the traditional fossil fuels are gradually exhausted and environmental pollution is becoming more serious. Current energy consumption has a significant impact on people's life and economy development. Therefore, the development of sustainable new and clean energy has been becoming an urgent and primary task. So high-efficient energy storage devices will play more significant role in human society [1-3]. Compared to traditional capacitors and batteries, supercapacitor is a new type of chemical power supply [4]. Supercapacitor has the characteristics of high specific capacitance, long cycle life and rapid charge/discharge rate. So supercapacitor is considered to be an ideal energy storage device.

At present, the studies on supercapacitors mainly focus on the development of electrode materials. Electrode materials play a decisive role in electrochemical properties [5]. So development materials with high specific capacitance, low cost, environmental protection and long life is crucial. As electrode materials, nickel-cobalt compounds have many advantages, including high rich redox reaction, specific capacitance and so on. They are becoming the hotspot of research [6]. Due to the structural characteristics and composition, metal-organic framework materials have been proved to be a perfect precursor for preparing transition metal compounds with good electrochemical properties [7, 8]. In particular, transition metal selenide has attracted much attention for its considerable theoretical capacitance as well as excellent conductivity [9-11]. However, the poor cycling stability of selenide hinders the promising application. In this work,

ZIF-67 is firstly synthesized, which then reacts with  $\text{Ni}(\text{NO}_3)_2 \cdot 6\text{H}_2\text{O}$  to produce the precursor containing nickel and cobalt. And then the precursor is converted into nickel-cobalt selenides through hydrothermal reaction. The effect of molar ratio of Co/Ni on the crystalline phase, morphology and electrochemical performance has been investigated. Results show that the selenides exhibit different crystalline phase and particles dispersion state under various molar ratio of Co/Ni, and the corresponding selenides show different electrochemical properties. At optimized molar ratio of Co/Ni, the selenides show high specific capacitance and long cycling stability.

## 2. Experimental section

Cobalt nitrate hexahydrate, 2-methyl imidazole, methanol, selenium powder, sodium borohydride, nickel nitrate hexahydrate, potassium chloride and potassium hydroxide were purchased from the National Pharmaceutical Group Chemical Reagent Co., Ltd. Self-made distilled water is used.

### 2.1. Synthesis of precursor

Firstly, ZIF-67 was synthesized according to the literature [12], which has been recorded in our previous work [13]. Then the obtained ZIF-67 was put into 15 mL methanol. And a certain amount of nickel nitrate hexahydrate was dissolved in 15 mL methanol, the molar ratio of Co/Ni was set at 3/1, 1/1 and 1/3, respectively. Then the latter was added to the former with ultrasonic treatment for 15 minutes. The obtained mixed solution was

put into a 50 ml Teflon-lined stainless-steel autoclave and set at 120 °C for 1 hour. After the reaction was completed, the precipitate was obtained through centrifuging and drying in vacuum at 40 °C for 8 hours.

## 2.2. Synthesis of selenides

0.16 g selenium powder and 0.23 g sodium borohydride were added to a three-mouth flask in the glove box to isolate oxygen. And then the above flask was kept at -10 °C in a digital refrigerated circulator. After three nitrogen replacements, 2 mL absolute ethanol, 38 mL oxygen-free water and 100 mg precursor were added to the above mixture. Then the above mixture was put into a 50 ml autoclave and kept at 180 °C for 4 h. Finally, the obtained samples were centrifuged, washed, and dried at 40 °C for 12 h in turn.

## 2.3. Electrochemical performance test

The electrochemical performance was tested through a three-electrode system at CHI 760E with 2.0 M KOH as electrolyte. The electrode materials were the prepared nickel-cobalt selenides, which were used to prepare working electrode, through our previous method [1]. Counter electrode was a platinum foil and the reference electrode was a standard saturated calomel electrode.

Specific capacitance of the electrode materials was evaluated from the galvanostatic charge/discharge curve with the equation (1), which has been recorded in our previous work [1].

$$C_m = \frac{i \times \Delta t}{\Delta V \times m} \quad (1)$$

## 3. Results and discussion

The crystalline structural of the samples has been investigated by XRD technique. In this work, ZIF-67 was prepared, and the corresponding XRD pattern has been indexed to ZIF-67 with high purity, as shown in our previous work [13]. Then Ni element was introduced to synthesize precursor. In presence of the precursor, selenium powder and sodium borohydride, nickel-cobalt selenides were fabricated through hydrothermal reaction. XRD patterns of the obtained nickel-cobalt selenides are shown in Fig. 1. For the sample NiCoSe-1, NiCoSe-2 and NiCoSe-3, the diffraction peaks are indexed with the CoSe<sub>2</sub> phase (PDF#03-065-3327), NiSe<sub>2</sub> phase (PDF#03-065-1843) and the Ni<sub>3</sub>Se<sub>4</sub> phase (PDF#01-089-2020), respectively. In briefly, the samples obtained at various molar ratio of Co/Ni show different

crystal phases, suggesting molar ratio of Co/ Ni affects the crystalline phases. ICP results show that the molar ratios of Co/Ni in NiCoSe-1, NiCoSe-2 and NiCoSe-3 are about 3: 1, 1:1 and 1:3, respectively, which are similar to those in the raw materials.

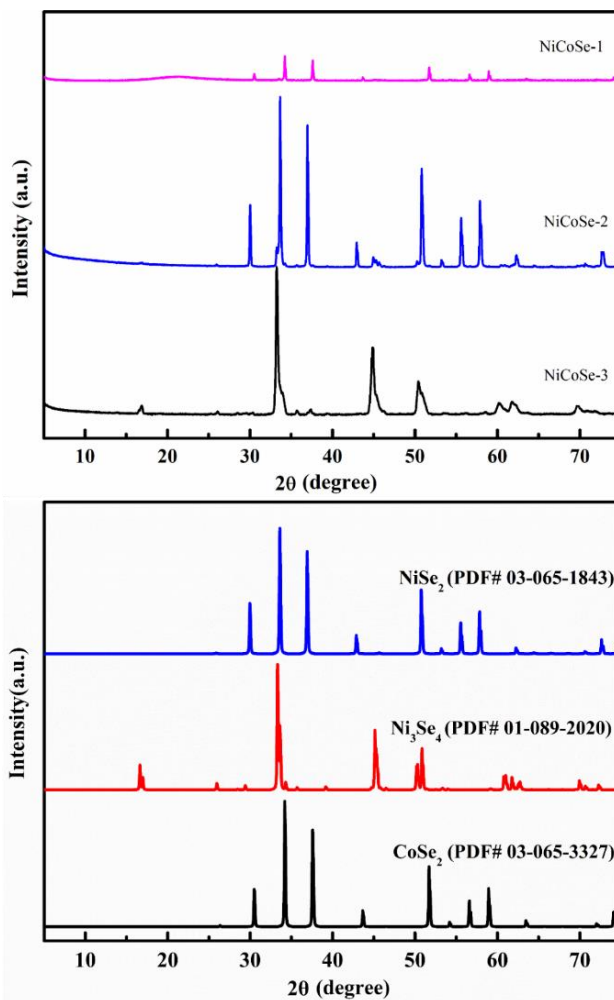


Fig. 1. The XRD patterns (color online)

Morphology of the obtained selenides is examined using SEM method. As shown in the Fig. 2a, amorphous particles appear in the sample NiCoSe-1 and there are gaps between the particles. Compared to the sample NiCoSe-1, the particle size of NiCoSe-2 is more uniform. And there are more gaps between the amorphous particles (Fig. 2b). As for the sample NiCoSe-3, amorphous particles pile up and lack space between each other (Fig. 2c).

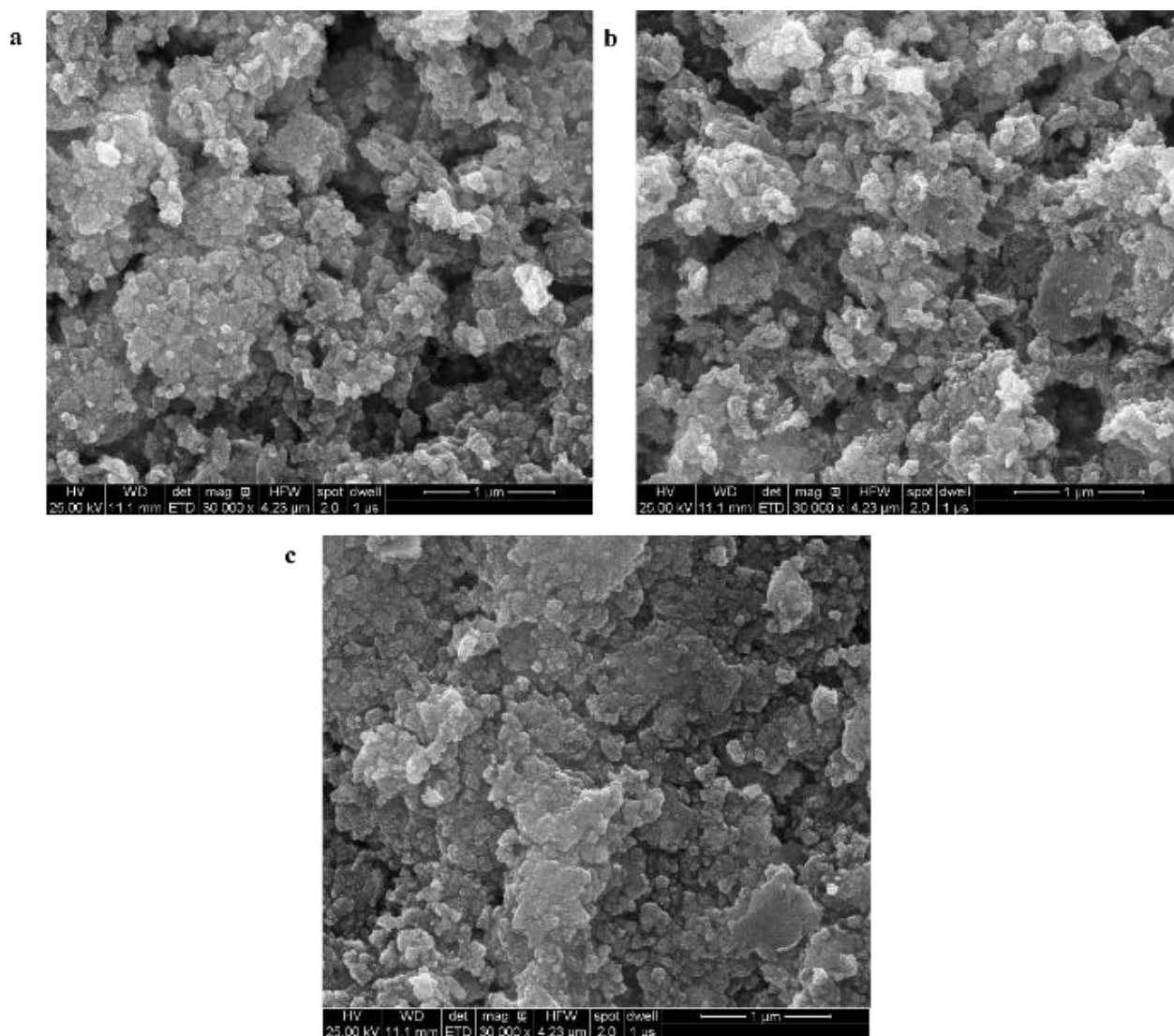


Fig. 2. SEM images of (a) NiCoSe-1, (b) NiCoSe-2 and (c) NiCoSe-3

The electrochemical properties of the synthesized selenides have been tested. CV curves of selenides at  $30 \text{ mV S}^{-1}$  are shown in the Fig. 3a. The selenides obtained at different molar ratio of Co/Ni show prominent redox peaks and good symmetry, suggesting the battery-like behavior [14, 15]. By comparing of CV curves of the above samples, it can be found that the CV curve area of NiCoSe-2 is biggest, showing the sample NiCoSe-2 possesses the highest specific capacitance. The above good properties might be ascribed to synergy effect between nickel and cobalt at the appropriate molar ratio [16-18]. As for the sample NiCoSe-2, the CV curves at various scan rates are shown in the Fig. 3b. As increasing scanning rate, the corresponding cathodic peak and anodic peak shift towards the negative potential and positive potential, respectively, which may be due to the polarization phenomenon. Impressively, even at  $50 \text{ mV s}^{-1}$ , cathodic peak and anodic peak are obvious, showing the fast process of charging and discharging.

The GCD curves of NiCoSe-2 at various current density are obtained. As show in the Fig. 3c, prominent

discharge platform appears in the GCD curve, showing the battery-like behavior [19] and corresponding to the appearance of redox peaks in CV curves. Even at high current density, the platform on GCD curve is obvious. The specific capacitance is shown in Fig. 3d. The samples show high mass specific capacitance at low current density. With the increase of current density from 1 to  $20 \text{ A g}^{-1}$ , the specific capacitance gradually decreases. According to the Fig. 3d, the sample NiCoSe-2 has the highest specific capacitance. It shows  $1234.2 \text{ F g}^{-1}$ ,  $1040.2 \text{ F g}^{-1}$ ,  $981.9 \text{ F g}^{-1}$ ,  $907.6 \text{ F g}^{-1}$ ,  $871.2 \text{ F g}^{-1}$ ,  $851.2 \text{ F g}^{-1}$  and  $706.8 \text{ F g}^{-1}$  at  $1 \text{ A g}^{-1}$ ,  $2 \text{ A g}^{-1}$ ,  $3 \text{ A g}^{-1}$ ,  $4 \text{ A g}^{-1}$ ,  $8 \text{ A g}^{-1}$ ,  $10 \text{ A g}^{-1}$  and  $20 \text{ A g}^{-1}$ , respectively. As for the sample NiCoSe-1, the specific capacitance is  $1001.1 \text{ F g}^{-1}$ ,  $924.2 \text{ F g}^{-1}$ ,  $856.7 \text{ F g}^{-1}$ ,  $860.5 \text{ F g}^{-1}$ ,  $792.9 \text{ F g}^{-1}$ ,  $768.9 \text{ F g}^{-1}$ ,  $624.6 \text{ F g}^{-1}$  at  $1 \text{ A g}^{-1}$ ,  $2 \text{ A g}^{-1}$ ,  $3 \text{ A g}^{-1}$ ,  $4 \text{ A g}^{-1}$ ,  $8 \text{ A g}^{-1}$ ,  $10 \text{ A g}^{-1}$  and  $20 \text{ A g}^{-1}$ , respectively. The specific capacitance of NiCoSe-3 is relative low, compared to that of NiCoSe-1 and NiCoSe-2. According to the above results, the molar ratio of Co/Ni in the nickel-cobalt selenides influences the electrochemical properties.

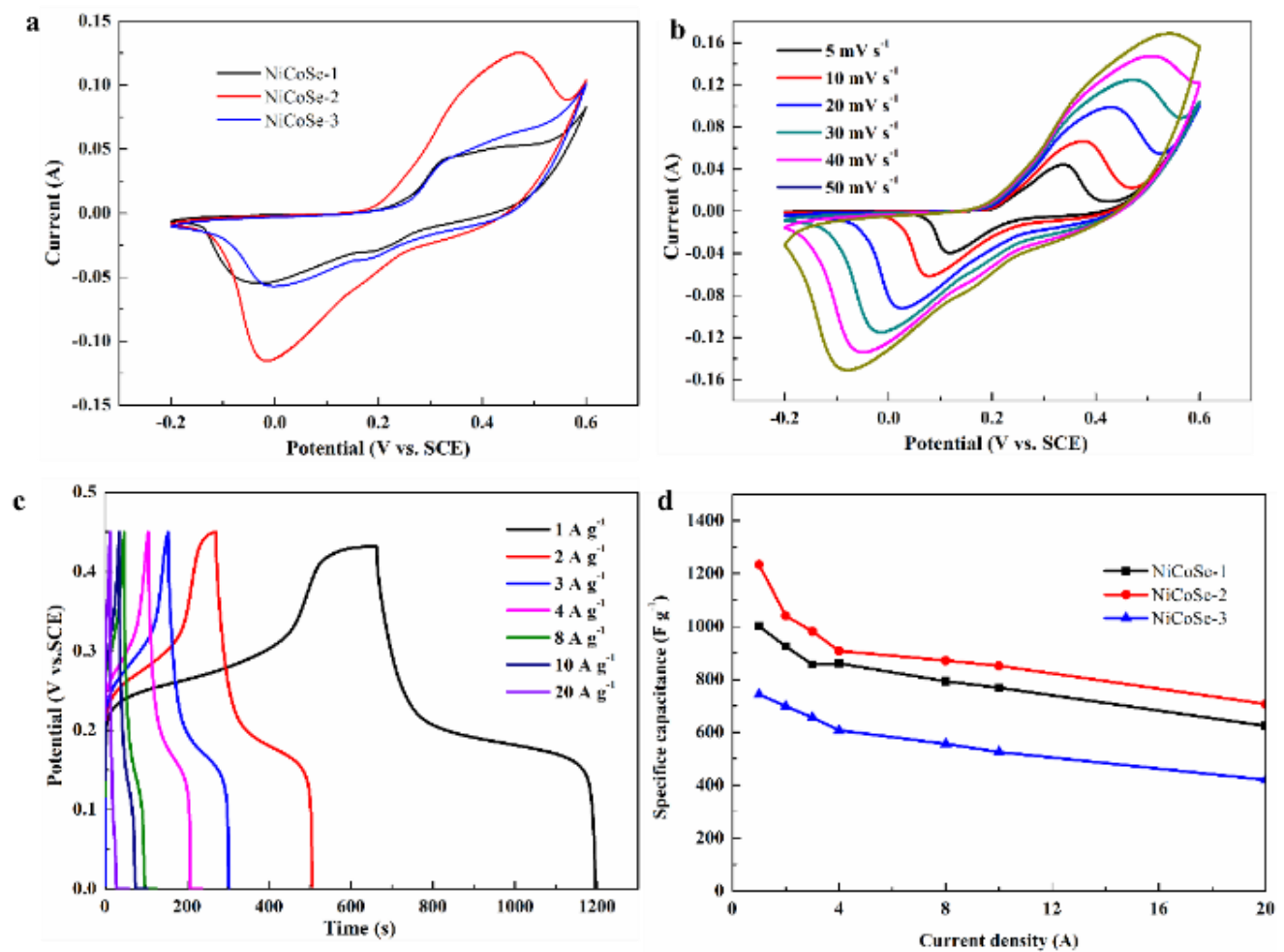


Fig. 3. (a) CV curves at  $30 \text{ mV s}^{-1}$  of NiCoSe-1, NiCoSe-2 and NiCoSe-3, (b) CV curves of NiCoSe-2, (c) GCD curves of NiCoSe-2, (d) mass-specific capacitance of samples (color online)

The cycling stability at current density of  $10 \text{ A g}^{-1}$  of NiCoSe-2 is shown in Fig. 4. Impressively, in the initial 2200 cycles, the capacitance increases gradually with the progress of charging/discharging. And the capacitance retention reaches 114.6 % at the 2200 cycle. Among 2200 to 4400 cycles, the capacitance retention is basically stable between 113.5 and 114.9 %. Then the specific capacitance retention decreases gradually. When the times of charge/discharge reach 10000 cycles, the specific capacitance retention rate still remains at 76.0 %. So the sample NiCoSe-2 shows stable cycling performance. As for the sample NiCoSe-2, the synergy effect brought out by the optimized molar ratio of Co to Ni (1/1) [20, 21], particles dispersion state and the appearance of gap between the particles may contribute to the wonderful electrochemical properties.

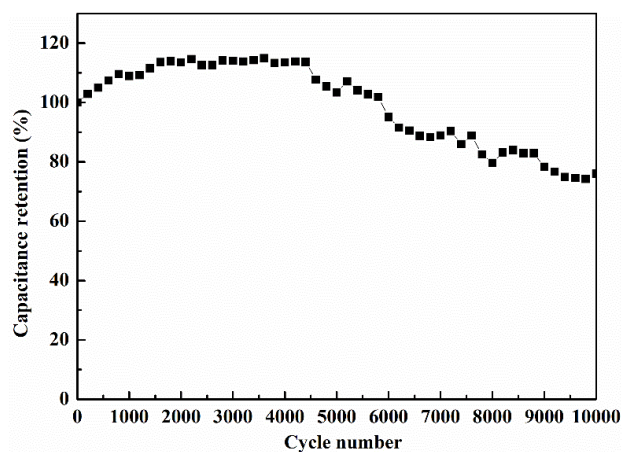


Fig. 4. Cycling performance of NiCoSe-2

#### 4. Conclusion

In conclusion, nickel-cobalt selenides were fabricated in this work. The effect of molar ratio of Co/Ni on the composition and microstructure of selenides was studied. It is found that the molar ratio of Co/Ni influences the crystalline phase and particles dispersion state of the selenides. And the samples obtained at various molar ratio of nickel/cobalt exhibit different electrochemical performance as supercapacitor electrode materials. Impressively, the sample NiCoSe-2 obtained under optimum molar ratio of Co/Ni (1/1) shows the best electrochemical performance. It shows  $1234.2 \text{ F g}^{-1}$  at  $1 \text{ A g}^{-1}$  and 76.0 % of the initial capacitance after 10000 cycles.

#### Acknowledgments

Financially supported by Shandong Provincial Natural Science Foundation (ZR2020MB079) and Key Research and Development Program of Shandong Province (2019GGX103011), Doctoral Program of Binzhou University (2021Y22) and Key Research and Development Program of Binzhou University (2020ZD05), National Undergraduate Training Program for Innovation and Entrepreneurship (S202110449185, X202110449434, X202110449435).

#### References

- [1] S. Xie, J. Gou, B. Liu, C. Liu, *Inorg. Chem. Front.* **5**(5), 1218 (2018).
- [2] D. Larcher, J. M. Tarascon, *Nat. Chem.* **7**(1), 19 (2015).
- [3] G. Wang, L. Zhang, J. Zhang, *Chem. Soc. Rev.* **41**(2), 797 (2012).
- [4] Y. Shao, M. F. El-Kady, J. Sun, Y. Li, Q. Zhang, M. Zhu, H. Wang, B. Dunn, R. B. Kaner, *Chem. Rev.* **118**(18), 9233 (2018).
- [5] C. Zhong, Y. Deng, W. Hu, J. Qiao, L. Zhang, J. Zhang, *Chem. Soc. Rev.* **44**(21), 7484 (2015).
- [6] H. Chen, L. Hu, M. Chen, Y. Yan, L. Wu, *Adv. Func. Mater.* **24**(7), 934 (2014).
- [7] B. Xu, H. Zhang, H. Mei, D. Sun, *Coordin. Chem. Rev.* **420**, 213438 (2020).
- [8] Z. Xiao, Y. Mei, S. Yuan, H. Mei, H. C. Zhou, *ACS Nano* **13**(6), 7024 (2019).
- [9] S. Xie, J. Gou, B. Liu, C. Liu, *J. Colloid. Interf. Sci.* **540**(22), 306 (2019).
- [10] C. Xia, H. Liang, J. Zhu, U. Schwingenschlöggl, H. N. Alshareef, *Adv. Energy Mater.* **7**(9), 1602089 (2017).
- [11] T. Chen, S. Li, J. Wen, P. Gui, Y. Guo, C. Guan, J. Liu, G. Fang, *Small* **14**(5), 1700979 (2018).
- [12] H. Hu, Bu Y. Guan, Xiong W. Lou, *Chem.* **1**(1), 102 (2016).
- [13] J. Gou, Y. Du, S. Xie, Y. Liu, X. Kong, *Inter. J. Hydrogen. Energ.* **44**(50), 27214 (2019).
- [14] P. Xu, J. Liu, P. Yan, C. Miao, K. Ye, K. Cheng, J. Yin, D. Cao, K. Lia, G. Wang, *J. Mater. Chem. A* **4**(13), 4920 (2016).
- [15] L. Li, J. Xu, J. Lei, J. Zhang, F. McLarnon, Z. Wei, N. Li, F. Pan, *J. Mater. Chem. A* **3**(5), 1953 (2015).
- [16] B. Liu, Y. F. Zhao, H. Q. Peng, Z. Y. Zhang, C. K. Sit, M. F. Yuen, T. R. Zhang, C. S. Lee, W. J. Zhang, *Adv. Mater.* **29**(19), 1606521 (2017).
- [17] X. Song, C. Huang, Y. Qin, H. Li, H. C. Chen, J. Mater. Chem. A **6**(33), 16205 (2018).
- [18] H. Chen, S. Chen, M. Fan, C. Li, D. Chen, G. Tian, K. Shu, *J. Mater. Chem. A* **3**(47), 23653 (2015).
- [19] S. Zhou, W. Wei, Y. Zhang, S. Cui, L. Mi, *Sci. Rep.-UK* **9**(1), 12727 (2019).
- [20] Y. Guo, X. Hong, Y. Wang, Q. Li, J. Meng, R. Dai, X. Liu, L. He, L. Mai, *Adv. Func. Mater.* **29**(24), 1809004 (2018).
- [21] Y. Huang, C. Yan, X. Shi, W. Zhi, Z. Li, Y. Yan, M. Zhang, G. Cao, *Nano Energy* **48**, 430 (2018).

\*Corresponding author: shenglixie@126.com,  
goujianxia@163.com